Biochemical and Biophysical Research Communications 454 (2014) 269–274

Contents lists available at ScienceDirect

Biochemical and Biophysical Research Communications

journal homepage: www.elsevier.com/locate/ybbrc

# Amino acid substitutions away from the RNase H catalytic site increase the thermal stability of Moloney murine leukemia virus reverse transcriptase through RNase H inactivation

Atsushi Konishi [a], Tetsuro Hisayoshi [a], Kanta Yokokawa [a], Verónica Barrioluengo [b], Luis Menéndez-Arias [b], Kiyoshi Yasukawa [a,*]

[a] Division of Food Science and Biotechnology, Graduate School of Agriculture, Kyoto University, Sakyo-ku, Kyoto 606-8502, Japan
[b] Centro de Biología Molecular "Severo Ochoa" (Consejo Superior de Investigaciones Científicas and Universidad Autónoma de Madrid), c/Nicolás Cabrera 1, Campus de Cantoblanco, 28049 Madrid, Spain

ARTICLE INFO

*Article history:*
Received 1 October 2014
Available online 17 October 2014

*Keywords:*
Moloney murine leukemia virus
Reverse transcriptase
RNase H activity
Template–primer
Thermostabilization

ABSTRACT

We have previously used site-directed mutagenesis to introduce basic residues (i.e., Arg; Lys) in the nucleic acid binding cleft of the Moloney murine leukemia virus reverse transcriptase (MMLV RT) in order to increase its template–primer (T/P) binding affinity. Three stabilizing mutations (i.e., E286R, E302K, and L435R) were identified (Yasukawa et al., 2010). Now, we studied the mechanism by which those mutations increase the thermal stability of the RT. The three single-mutants (E286R, E302K, and L435R), an RNase H-deficient MMLV RT (carrying the RNase H-inactivating mutation D524A), a quadruple mutant (E286R/E302K/L435R/D524A, designated as MM4) and the wild-type enzyme (WT) were produced in *Escherichia coli*. All RTs exhibited similar dissociation constants ($K_d$) for heteropolymeric DNA/DNA (2.9–6.5 nM) and RNA/DNA complexes (1.2–2.9 nM). Unlike the WT, mutant enzymes (E286R, E302K, L435R, D524A, and MM4) were devoid of RNase H activity, and were not able to degrade RNA in RNA/DNA complexes. These results suggest that the mutations, E286R, E302K, and L435R increase the thermostability of MMLV RT not by increasing its affinity for T/P but by abolishing its RNase H activity.



## 1. Introduction

Retroviral reverse transcriptase (RT) [EC 2.7.7.49] possesses RNA- and DNA-dependent DNA polymerase as well as RNase H activities. Moloney murine leukemia virus (MMLV) RT is extensively used in cDNA synthesis [1]. MMLV RT is a 75-kDa monomer, comprised of the fingers, palm, thumb, and connection subdomains and an RNase H domain [2,3]. The active site of the DNA polymerase activity is located in the palm subdomain while residues in the fingers and thumb subdomains participate in nucleotide and primer binding.

Improving the efficiency of the RT DNA polymerase activity at high temperatures has been an important area of research in biotechnology. Available RTs efficient at high temperatures have been obtained by inactivating their RNase H activity [4–8], or by improving template–primer binding affinity [9–11]. Random mutagenesis [12,13] and rational design [9–11] have been used to generate those RT variants. Thermostable RTs from MMLV [4–6], avian myeloblastosis virus (AMV) [5,7], and human immunodeficiency virus type 1 (HIV-1) [8] have been generated by deleting the RNase H domain [5] or by site-directed mutagenesis of the catalytic residues of the RNase H activity [6–8]. Using random mutagenesis, Arezi and Hogrefe identified five stabilizing mutations of MMLV RT (i.e., E69K, E302R, W313F, L435G, and N454K) [12], and Baranauskas et al. identified another five (i.e., L139P, D200N, T330P, L603W, and E607K) [13]. The obtained RTs with mutations E69K/E302R/W313F/L435G/N454K [12] and L139P/D200N/T330P/L603W/E607K [13] exhibited remarkable thermostability. In the case of E69K/E302R/W313F/L435G/N454K, thermostabilization has been attributed to an increase in template–primer (T/P) binding affinity.

We have previously identified five stabilizing mutations (E286R, E302K, L435R, V433K, and V433R) [9,10] by introducing basic residues in the predicted nucleic acid binding cleft of the RT. In those studies, we hypothesized that the introduction of

*Abbreviations:* HIV-1, human immunodeficiency virus type 1; MMLV, Moloney murine leukemia virus; RNase H, ribonuclease H; RT, reverse transcriptase; PAGE, polyacrylamide gel electrophoresis.

* Corresponding author. Fax: +81 75 753 6265.
*E-mail address:* yasukawa@kais.kyoto-u.ac.jp (K. Yasukawa).

http://dx.doi.org/10.1016/j.bbrc.2014.10.044
0006-291X/

positive charges increases the thermostability of MMLV RT by improving its ability to bind the T/P that is negatively charged. Now, we show evidence that reveals that mutations E286R, E302K, and L435R responsible for the higher thermal stability of the RT do not affect T/P binding affinity, but abolish the RNase H activity of the polymerase.

## 2. Materials and methods

### 2.1. Expression and purification of recombinant MMLV RT

Recombinant MMLV RT was prepared as described previously [6]. *Escherichia coli* strain BL21(DE3) was transformed with the pET-22b(+) plasmid (Merck Bioscience, Tokyo, Japan) harboring the nucleotide sequence encoding the MMLV RT with a C-terminal $(His)_6$-tag. *E. coli* cells were harvested from a 2-liter culture, and resuspended in 20 ml of 20 mM potassium phosphate (pH 7.2) buffer, containing 2 mM dithiothreitol (DTT) and 10% (v/v) glycerol (buffer A). After adding 1 mM phenylmethylsulfonyl fluoride (PMSF) to buffer A, cells were sonicated. After centrifugation at 20,000×*g* for 40 min, the supernatant was collected and applied to a column [25 mm (inner diameter) × 120 mm] packed with Toyopearl DEAE-650 M gel (Tosoh, Tokyo, Japan), previously equilibrated with buffer A. The column was washed with 80 ml of buffer A containing 120 mM NaCl and eluted with buffer A containing 300 mM NaCl, to which saturated $(NH_4)_2SO_4$ was added to a final 40% saturation. After centrifugation at 20,000×*g* for 30 min, the pellet was collected and dissolved in 10 ml of buffer A containing 500 mM NaCl. After centrifugation at 20,000×*g* for 5 min, the supernatant was applied to the column packed with $Ni^{2+}$-Sepharose™ (HisTrap HP 1 ml, GE Healthcare, Buckinghamshire, UK), previously equilibrated with buffer A. The column was washed with 50 ml of 50 mM Tris–HCl (pH 8.3) buffer, containing 200 mM KCl, 2 mM DTT, 10% glycerol, and 50 mM imidazole, and the RT was eluted with 3 ml of 50 mM Tris–HCl (pH 8.3) buffer, containing 200 mM KCl, 2 mM DTT, 10% glycerol, and 500 mM imidazole. The eluate was then applied to the column packed with Sephadex G-25 (PD-10, GE Healthcare), previously equilibrated with 50 mM Tris–HCl (pH 8.3), containing 200 mM KCl and 50% glycerol (buffer B). The column was washed and eluted with the same buffer. This sequential chromatography procedures consisting of the $Ni^{2+}$-Sepharose™ column and the Sephadex G-25 column were repeated two more times. The eluate at the final step was further purified by chromatography on the Sephadex G-25 column. Purified MMLV RT was stored at −80 °C before use. MMLV RT concentration was determined using the Protein Assay CBB Solution (Nacalai Tesque, Kyoto, Japan) using bovine serum albumin as standard.

### 2.2. Thermal inactivation of MMLV RT

MMLV RT (100 nM) in 10 mM potassium phosphate (pH 7.6) buffer, containing 2 mM DTT, 0.2% Triton X-100, and 10% glycerol was incubated in the presence and absence of 28 μM poly(rA)-$p(dT)_{15}$ at 50 °C for 10 min followed by incubation on ice for 30 min. The residual DNA polymerase activity of MMLV RT was measured as described previously [9]. Briefly, the reaction was carried out in 25 mM Tris–HCl (pH 8.3) buffer, containing 50 mM KCl, 2 mM DTT, 5 mM $MgCl_2$, 25 μM poly(rA)-$p(dT)_{15}$ (this concentration is expressed as that of $p(dT)_{15}$), 0.2 mM [$^3$H]dTTP, and 10 nM MMLV RT at 37 °C. Aliquots of 20 μl were collected at different times and immediately spotted onto glass microfiber filters GF/C of 2.5 cm (Whatman, Middlesex, UK). Unincorporated [$^3$H]dTTP was removed by three washes with chilled 5% (w/v) trichloroacetic acid for 10 min each followed by one wash with chilled 95% ethanol. The amounts of [$^3$H]dTTP incorporated were determined by scintillation counting in 2.5 ml of Ecoscint H solution (National Diagnostics, Atlanta, GA) using a LSC-5100 apparatus (Aloka, Mitaka, Japan), and the initial reaction rate was determined.

### 2.3. Determination of dissociation constants ($K_d$) of RT–T/P complexes

The 31T(DNA) or the 31T(RNA) and the 21P-C(DNA) labelled with [γ-$^{32}$P]ATP (PerkinElmer, Boston, MA) at its 5′-terminus were annealed to generate T/Ps 31T(DNA)/[$^{32}$P]21P-C(DNA) and 31T(RNA)/[$^{32}$P]21P-C(DNA). MMLV RTs (12 nM) were pre-incubated with various concentrations of either of the two duplexes (2–40 nM) at 37 °C for 10 min in 20 μl of 50 mM Tris–HCl (pH 8.0) buffer, containing 50 mM KCl. Reactions were initiated by adding 20 μl of 50 mM Tris–HCl (pH 8.0) buffer, containing 20 mM dTTP, 50 mM KCl, 30 mM $MgCl_2$, and 20 μM 31T(DNA)/21P-C(DNA). The 31T(DNA)/21P-C(DNA) at high concentration (20 μM) binds unbound RT as well as RT that dissociates from DNA/DNA or RNA/DNA duplexes, preventing further RT binding to labelled T/Ps. Aliquots of 4 μl were removed at 15, 30, and 45 s, and immediately quenched with 4 μl of sample-loading buffer (10 mM EDTA, 90% (v/v) formamide, 3 mg/ml xylene cyanol FF, 3 mg/ml bromophenol blue, and 50 μM 31T(DNA)/21P-C(DNA)). The reaction products were analyzed by denaturing 20% polyacrylamide gel electrophoresis and quantified with a BAS-2500 scanner (Fujifilm, Tokyo, Japan) using the program Multi Gauge version 2.2 (Fujifilm). For each reaction, the percentage of elongated primer was plotted against the incubation times and the data were fit to a linear equation. As the concentration of template–primer is well above the dissociation constant of MMLV RT, $K_d$, under this assay conditions, the RT–T/P concentration, [RT–T/P], in the preincubated mixture was calculated from the *y*-intercept that represents the amount of RT bound to template–primer at time zero. The $K_d$ values were determined by fitting the data thus obtained to Eq. (1),

$$[RT-T/P] = 0.5 \times \left(K_d + [RT]_o + [T/P]_o\right) - 0.5 \times \left\{\left(K_d + [RT]_o + [T/P]_o\right)^2 - 4[RT]_o[T/P]_o\right\}^{0.5} \quad (1)$$

where $K_d$ is the dissociation constant of MMLV RT with T/P, and $[RT]_o$ and $[T/P]_o$ is the initial RT and T/P concentration, respectively, in the preincubated mixture. The relative RT–T/P concentration, defined as the ratio of the respective RT–T/P concentration to the maximum values obtained, was plotted as a function of the initial T/P concentration.

### 2.4. Extension of primers in the absence of one dNTP

The DNA polymerase activity of MMLV RT in the absence of one dNTP was determined using a method previously described [14]. Briefly, the reaction (40 μl) was carried out at 37 °C in 50 mM Tris–HCl (pH 8.0) buffer, containing 50 mM KCl, 15 mM $MgCl_2$, 150 nM MMLV RT, 20 nM D2-47(DNA)/[$^{32}$P]PG5-25(DNA), and 250 μM each dNTP. The reaction was stopped after a two-hour incubation, and the reaction products were analyzed as described above (Section 2.3).

### 2.5. RNase H activity assay

The RNase H activity of MMLV RT was determined as described previously [15]. Briefly, four RNA/DNA duplexes were prepared. The reaction (40 μl) was carried out in 50 mM Tris–HCl (pH 8.0) buffer, containing 50 mM KCl, 15 mM $MgCl_2$, 150 nM MMLV RT, and 20 nM [$^{32}$P]31T(RNA)/21P-C(DNA), [$^{32}$P]D2-47(RNA)/PG5-25(DNA), [$^{32}$P]D2-25(RNA)/PG5-25(DNA), or [$^{32}$P]31T(RNA)/15P(DNA) at 37 °C for 0–40 min. Then aliquots were removed at

different times (0.25, 0.5, 2, 4, 20, and 40 min), and the reaction products were analyzed as described above (Section 2.3).

## 3. Results

### 3.1. Preparation and characterization of MMLV RT

We previously generated four thermostable MMLV RT variants by introducing single amino acid substitutions (E286R, E302K, L435R, and D524A) as well as one quadruple variant (E286R/E302K/L435R/D524A, designated as MM4) [9]. Wild-type enzyme (WT) and all mutant RTs were expressed in *E. coli* and purified to homogeneity. RTs were judged to be pure by SDS–PAGE, and the $M_r$ values obtained were around 75,000 (Fig. 1A).

DNA polymerase activities of all enzymes were determined at 37 °C after incubation at 50 °C for 10 min in the presence and absence of T/P (Fig. 1B). Each enzyme exhibited higher relative activity in the presence of T/P than in its absence, and all variants exhibited higher relative activities than WT both in the presence and the absence of T/P. These results are in agreement with those published in our previous report [9].

We measured UV, CD, and fluorescence spectra of the purified enzymes. All enzymes exhibited similar UV spectra with maximum absorbance at 275 nm (Fig. S1A). On CD spectroscopy, all RTs exhibited negative ellipticities at around 202–250 nm with minimum values around 208 and 222 nm (Fig. S1B). At excitation wavelength of 280 and 295 nm, all RTs exhibited emission fluorescence spectra with maximum intensities at 338 nm (Fig. S1C). No appreciable changes were observed in each spectra between WT and variants.

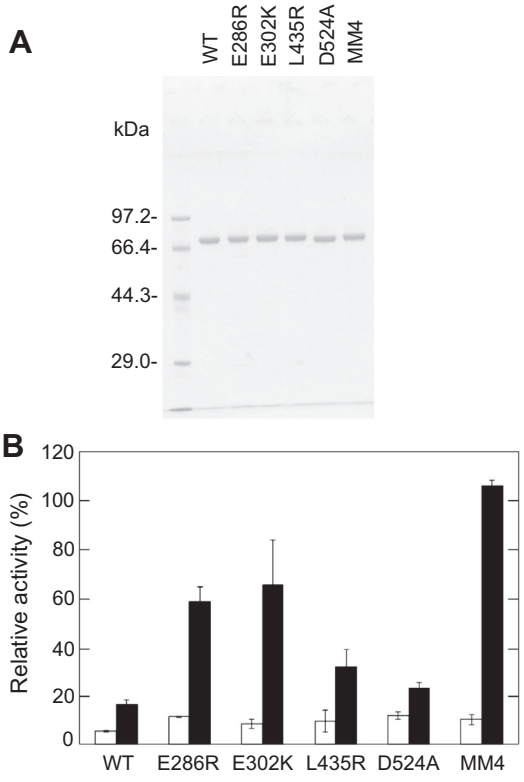


**Fig. 1.** Purification and characterization of MMLV RT. (A) SDS–PAGE under reducing conditions. Enzyme (1.2 μg) was applied to each lane. A Coomassie Brilliant Blue-stained 10% SDS–polyacrylamide gel is shown. (B) Thermal inactivation of MMLV RT. Enzyme was incubated at 50 °C for 10 min in the presence (black bar) and the absence (whilte bar) of poly(rA)-p$(dT)_{15}$. Then, the dTTP incorporation reaction using poly(rA)-p$(dT)_{15}$ as T/P was carried out at 37 °C. The relative activity was defined as the ratio of the initial reaction rate with heat treatment to that without it. Represented values were obtained from at least three independent experiments.

### 3.2. Effect of stabilizing mutations on the affinities of MMLV RT for T/P

In order to test whether individual mutations such as E286R, E302K, and L435R would affect T/P binding affinity, we determined the dissociation constants ($K_d$) of RT–T/P complexes. RTs were preincubated with various concentrations of radiolabelled T/P to form an RT–T/P complex. The reaction was initiated by adding dTTP, $Mg^{2+}$, and an excess of unlabelled T/P, and the products were analyzed. Fig. 2 shows the relative concentration of the RT–T/P complex *versus* the total T/P concentration in the preincubated mixture. Saturation curves were obtained for DNA/DNA (Fig. 2A) and RNA/DNA (Fig. 2B) duplexes. The $K_d$ values obtained with the DNA/DNA duplex and RTs WT, E286R, E302K, L435R, D524A, and MM4 were 2.9 ± 0.3, 3.5 ± 0.6, 6.5 ± 1.2, 5.4 ± 0.5, 3.3 ± 0.4, and 2.9 ± 0.3 nM, respectively, and the values obtained with the RNA/DNA duplex were 2.0 ± 0.3, 1.7 ± 0.2, 2.9 ± 0.3, 2.7 ± 0.4, 2.6 ± 0.2,

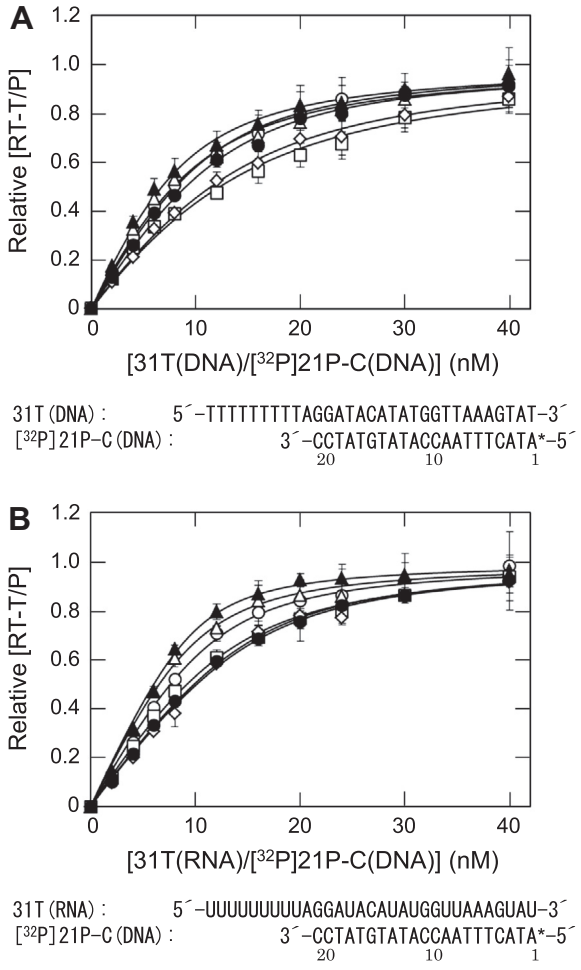


**Fig. 2.** Dissociation equilibrium of WT and mutant RTs with DNA/DNA and RNA/DNA complexes. WT and mutant RTs were preincubated with various concentrations of 31T(DNA)/[$^{32}$P]21P-C(DNA) (A) or 31T(RNA)/[$^{32}$P]21P-C(DNA) (B) at 37 °C for 10 min. DNA polymerization reactions were initiated by adding dTTP and unlabelled 31T(DNA)/21P-C(DNA). The initial concentrations of RT, dTTP, and unlabelled 31T(DNA)/21P-C(DNA) in the reaction were 6 nM, 10 mM, and 40 μM, respectively. The solid line is the best fit of the data to Eq. (1). The asterisk indicates the labelled nucleotide with [γ-$^{32}$P]ATP. Symbols: WT, open circle; E286R, open triangle; E302K, open square; L435R, open diamond; D524A, closed circle; and MM4, closed triangle.

and 1.2 ± 0.2 nM, respectively. These data indicate that WT and mutant RTs have similar binding affinities for T/P. The results also show that the binding affinities of MMLV RTs for the RNA/DNA duplex ($K_d$ values of 1.2–2.9 nM) are slightly higher than for the DNA/DNA duplex (2.9–6.5 nM).

### 3.3. Effect of the stabilizing mutations on the fidelity of MMLV RT

The effects of stabilizing mutations on the fidelity of MMLV RT were determined by measuring primer extension in the absence of one dNTP (Fig. 3). In the presence of all four dNTPs, fully-extended products of 47-nucleotides (nt) were obtained with all enzymes. In the absence of dGTP, the same result was obtained, compatible with the sequence of D2-47/PG5-25 in which dGTP is not required for faithful extension. When dATP was absent, in WT, E286R, L435R, and D524A, the intensities of the bands corresponding to 42- and 43-nt products were similar, while in reactions carried out with mutants E302K and MM4, the intensity of the 42-nt band was stronger than the intensity of the 43-nt band. This result is consistent with a lower misincorporation of A at position 43, by mutant E302K, suggesting that this mutation increases the fidelity of MMLV RT, while E286R, L435R, and D524A do not.

### 3.4. Effect of the stabilizing mutations on the RNase H activities of MMLV RT

It is known that the loss of RNase H activity caused by the mutation of the catalytic residue, Asp524, increases the stability of the RNA in reverse transcription reactions and improves the efficiency of the DNA polymerase activity [5]. In order to determine whether the three stabilizing mutations affect the RNase H activity, we measured the RNase H activities of WT and mutant enzymes with the RNA/DNA hybrid, [$^{32}$P]31T(RNA)/21P-C(DNA), consisting of 31-nt RNA and 21-nt DNA as the substrate (Fig. 4A). In reactions carried out with WT RT, evidence of cleavage was demonstrated by the presence of RNA bands of 28-nt or smaller, indicating that the RNA strand of the hybrid was first cleaved at the position of 18-bp upstream of the primer 3'-terminus. As expected, in D524A and MM4 of which the catalytic residue for RNase H activity, Asp524, is mutated to Ala, RNA remained undegraded. Unexpectedly, the mutants E286R, E302K, and L435R did not show RNase H activity, and RNA templates remained uncleaved after 40-min incubation at 37 °C (Fig. 4A).

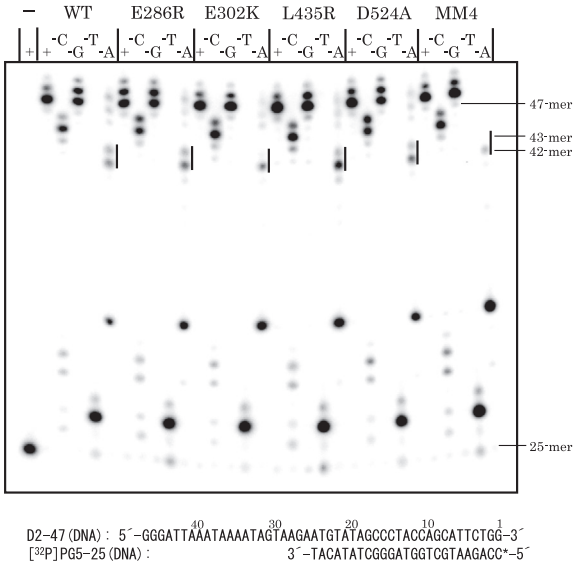


**Fig. 3.** Primer extension in the absence of one nucleotide. Reactions were carried out at 37 °C for 2 h with 150 nM MMLV RT, 20 nM D2-47(DNA)/[$^{32}$P]PG5-25(DNA), and 250 μM each dNTP. Lanes marked with + indicate that all four nucleotides were included in the dNTP mix. The lanes marked with -C, -G, -T, and -A indicate that three nucleotides except dCTP, dGTP, dTTP, or dATP, respectively, were included. Specific bands corresponding to products of 42- and 43-nucleotides are indicated.

In reactions carried out with HIV-1 RT, the RNA strand of an RNA/DNA hybrid is cleaved at a position of 16-bp upstream of the primer 3'-terminus [16], and that such T/P binds HIV-1 RT at its DNA polymerase and RNase H active sites [17], suggesting that the RNase H activity of MMLV RT varies depending on RNA/DNA hybrid species. To address this possibility, we used three additional RNA/DNA hybrids ([$^{32}$P]D2-47(RNA)/PG5-25(DNA) (Fig. 4B), [$^{32}$P]D2-25(RNA)/PG5-25(DNA) (Fig. 4C), and [$^{32}$P]31T(RNA)/15P(DNA)) (Fig. 4D). These T/Ps were designed to bind the DNA polymerase and RNase H active sites simultaneously, only the RNase H active site due to the lack of primer 3'-terminus, and either of the two active sites but not both simultaneously due to the usage of a shorter primer, respectively. With all RNA/DNA hybrid species, RNAs remained uncleaved in reactions catalyzed by all mutant RTs. This clearly indicates that mutations E286R, E302K, and L435R abrogate the RNase H activity.

## 4. Discussion

In this study, we demonstrate that the three stabilizing mutations (E286R, E302K, and L435R) eliminate the RNase H activity of MMLV RT. The crystal structure of the full-length enzyme has not been determined. Crystal structures of the polymerase domains of MMLV RT and the closely related xenotropic murine leukemia virus-related virus (XMRV) RT have been partially determined [2,18]. These structures reveal the common fold consisting of fingers, palm, thumb, and connection subdomains found in HIV-1 RT. On the other hand, the structures of the isolated RNase H domains of the MMLV RT and XMRV RT have also been determined [19,20]. Molecular models of MMLV RT suggest that the RNase H domain of MMLV RT is positioned far from the fingers/palm/thumb subdomain, like in the structure of the p66 subunit of HIV-1 RT [2,3]. Based on those models, it has been suggested that the RNase H domain alters the trajectory of the T/P, affecting the DNA polymerase activity [2,3]. Moreover, it has been reported that the DNA polymerase activity of a MMLV RT variant lacking the RNase H domain was considerably reduced [21].

Amino acid sequence identity between MMLV and XMRV RTs is around 95% [22]. The structure of the polymerase domain of XMRV RT bound to an RNA/DNA complex [18] reveals that Glu302 interacts with the T/P, but Glu286 and Leu435 are away from the nucleic acid binding cleft and long-distance effects appear to be responsible for the lack of RNase H activity of the corresponding mutants (Fig. S2).

In addition, the results of fidelity assays show that mutations that increase the thermal stability of the MMLV RT have a relatively minor effect on the accuracy of the polymerase. Among the studied mutations, only E302K produced a very modest improvement in the fidelity of the enzyme, detected only at selected sites in primer extension assays carried out in the absence of one nucleotide (Fig. 3).

In our study, all variants lacked RNase H activity, as demonstrated using four different RNA/DNA substrates. Two of them were designed with a template overhang to cover the DNA polymerase and the RNase H active sites simultaneously (Fig. 4A and B), a third substrate lacks the overhang and would bind only to the RNase H active site (Fig. 4C), while the fourth one is expected to bind any of the two active sites, but not both simultaneously, due to the relatively short distance between the 3′ end of the DNA primer and the putative RNase H cleavage site (Fig. 4D).

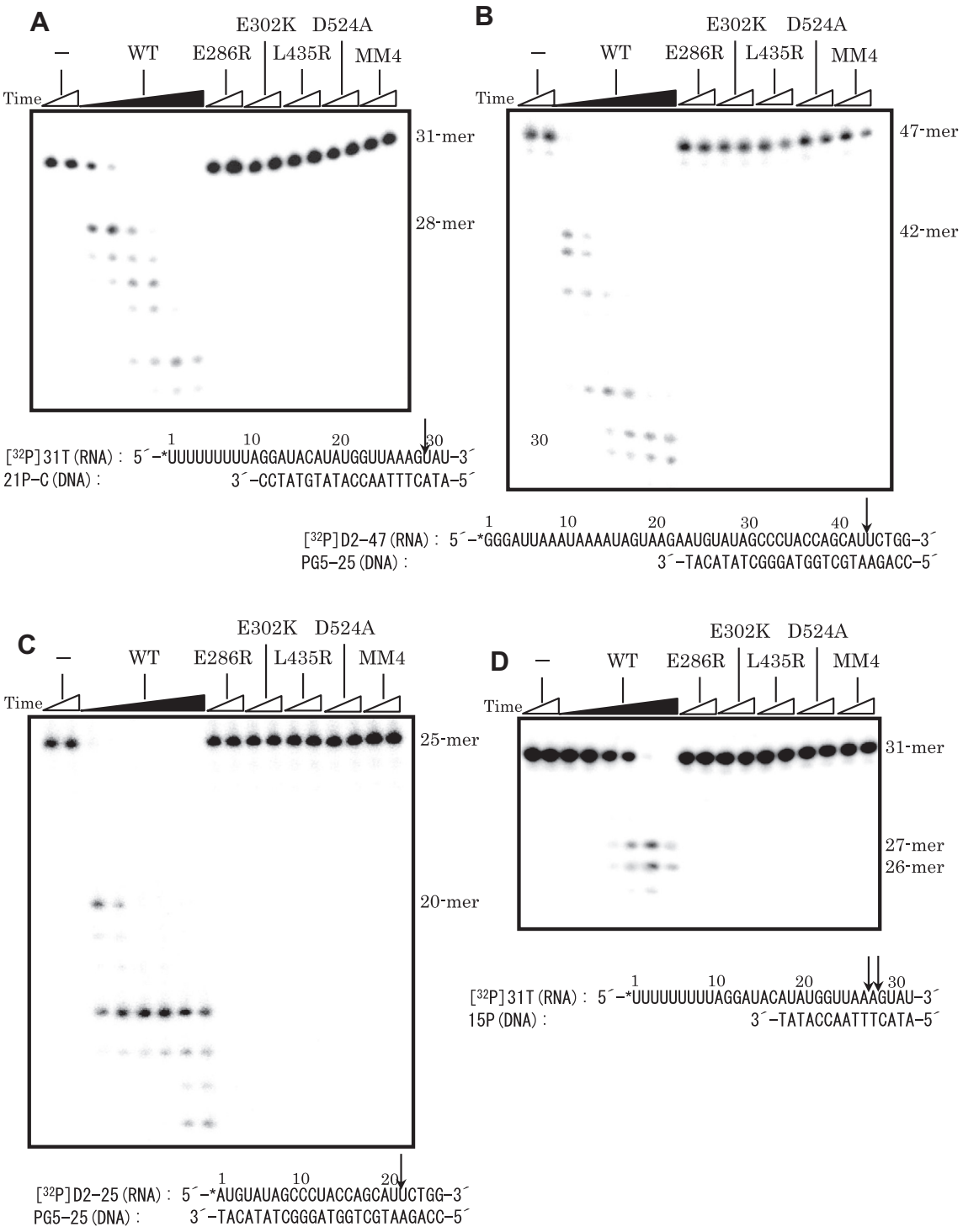


**Fig. 4.** RNase H activity. Reactions were carried out at 37 °C for 0–40 min in the presence of 20 nM labelled T/P and 0 or 150 nM RT. The arrows indicate the cleavage sites. Labelled T/P: (A) [$^{32}$P]31T(RNA)/21P-C(DNA); (B) [$^{32}$P]D2-47(RNA)/PG5-25(DNA); (C) [$^{32}$P]D2-25(RNA)/PG5-25(DNA); (D) [$^{32}$P]31T(RNA)/15P(DNA). The asterisk indicates the position of the $^{32}$P label. Time points were 0.25, 0.50, 2.0, 4.0, 20, and 40 min for WT and 0.25 and 40 min for mutant RTs.

Taking into account the structures of those substrates, we suggest that the three stabilizing mutations would alter the trajectory of the T/P and prevent its proper binding at the RNase H active site, leading to the loss of the RNase H activity. This is in contrast to the case with the mutation of the catalytic residue for the RNase H activity, Asp524. In this case, the RNase H active site cannot bind $Mg^{2+}$, leading to the loss of RNase H activity. In addition, it should be mentioned that the rate of the degradation reaction observed with the WT RT and the substrate [$^{32}$P]D2-25(RNA)/PG5-25(DNA) (Fig. 4C) is similar to rates calculated from assays shown in Fig. 4A and B, suggesting the possibility that the substrate used in Fig. 4C binds both the DNA polymerase and RNase H active sites simultaneously.

In this study, we also suggest that the three stabilizing mutations increase the thermostability of MMLV RT not by increasing its affinity for the T/P but by abolishing its RNase H activity. Although it has been reported that the thermostabilities of MMLV, AMV, and HIV-1 RTs are improved by the loss of the RNase H

activity through mutagenesis of catalytic residues [4–8], the mechanism is unknown. Goedken and Marqusee reported that in the CD analysis of the reversible unfolding of the isolated RNase H domain of MMLV RT (Pro515-Leu671), the midpoint denaturation temperature of D524N was higher by 10 °C than that of the WT RT, suggesting that the substitution of Asp524 eliminates the RT's RNase H activity, leading to an increase in the enzyme's intrinsic thermostability as a result of a structural change [23]. In the cases of E286R, E302K, and L435R, it was first thought that the observed higher thermostability was due to the increase in the T/P binding affinity [9]. However, this has been challenged by our data showing that WT and mutant RTs exhibit similar $K_d$ values (Fig. 2). As in the case of D524A, amino acid changes E286R, E302K, and L435R increase the RT's intrinsic thermal stability. Those mutations outside the RNase H catalytic site abolish the RNase H activity of the enzyme but do not affect its affinity for T/P.

## Acknowledgments

This study was supported in part by Grants-in-Aid for Scientific Research (No. 21580110 to K.Y.) and for JSPS Fellows (No. 25-1955 to A.K.) from the Japan Society for the Promotion of Science (JSPS). Work in Madrid has been partially supported by Spanish Government grants BIO2010-15542, BIO2013-48788-C2-1-R, and an institutional grant of Fundación Ramón Areces. L.M.-A. was recipient of an invitation short-term fellowship of the JSPS (FY2012).

## Appendix A. Supplementary data

Supplementary data associated with this article can be found, in the online version, at http://dx.doi.org/10.1016/j.bbrc.2014.10.044.

## References

[1] A.R. Kimmel, S.L. Berger, Preparation of cDNA and the generation of cDNA libraries: overview, Methods Enzymol. 152 (1987) 307–316.
[2] D. Das, M.M. Georgiadis, The crystal structure of the monomeric reverse transcriptase from Moloney murine leukemia virus, Structure 12 (2004) 819–829.
[3] M.L. Coté, M.J. Roth, Murine leukemia virus reverse transcriptase: structural comparison with HIV-1 reverse transcriptase, Virus Res. 134 (2008) 186–202.
[4] M.L. Kotewicz, J.M. D'Alessio, K.M. Driftmier, K.P. Blodgett, G.F. Gerard, Cloning and overexpression of Moloney murine leukemia virus reverse transcriptase in *Escherichia coli*, Gene 35 (1985) 249–258.
[5] G.F. Gerard, R.J. Potter, M.D. Smith, K. Rosenthal, G. Dhariwal, J. Lee, D.K. Chatterjee, The role of template–primer in protection of reverse transcriptase from thermal inactivation, Nucleic Acids Res. 30 (2002) 3118–3129.
[6] M. Mizuno, K. Yasukawa, K. Inouye, Insight into the mechanism of the stabilization of Moloney murine leukaemia virus reverse transcriptase by eliminating RNase H activity, Biosci. Biotechnol. Biochem. 74 (2010) 440–442.
[7] A. Konishi, K. Yasukawa, K. Inouye, Improving the thermal stability of avian myeloblastosis virus reverse transcriptase α-subunit by site-directed mutagenesis, Biotechnol. Lett. 34 (2012) 1209–1215.
[8] K. Nishimura, M. Shinomura, A. Konishi, K. Yasukawa, Stabilization of human immunodeficiency virus type 1 reverse transcriptase by site-directed mutagenesis, Biotechnol. Lett. 35 (2013) 2165–2175.
[9] K. Yasukawa, M. Mizuno, A. Konishi, K. Inouye, Increase in thermal stability of Moloney murine leukaemia virus reverse transcriptase by site-directed mutagenesis, J. Biotechnol. 150 (2010) 299–306.
[10] A. Konishi, X. Ma, K. Yasukawa, Stabilization of Moloney murine leukemia virus reverse transcriptase by site-directed mutagenesis of the surface residue Val433, Biosci. Biotechnol. Biochem. 78 (2014) 75–78.
[11] T. Matamoros, V. Barrioluengo, D. Abia, L. Menéndez-Arias, Major groove binding track residues of the connection subdomain of human immunodeficiency virus type 1 reverse transcriptase enhance cDNA synthesis at high temperatures, Biochemistry 52 (2013) 9318–9328.
[12] B. Arezi, H. Hogrefe, Novel mutations in Moloney murine leukemia virus reverse transcriptase increase thermostability through tighter binding to template–primer, Nucleic Acids Res. 37 (2009) 473–481.
[13] A. Baranauskas, S. Paliksa, G. Alzbutas, M. Vaitkevicius, J. Lubiene, V. Letukiene, S. Burinskas, G. Sasnauskas, R. Skirgaila, Generation and characterization of new highly thermostable and processive M-MuLV reverse transcriptase variants, Protein Eng. Des. Sel. 25 (2012) 657–668.
[14] M. Gutiérrez-Rivas, Á. Ibáñez, M.A. Martínez, E. Domingo, L. Menéndez-Arias, Mutational anlaysis of Phe160 within the "palm" subdomain of human immunodeficiency virus type 1 reverse transcriptase, J. Mol. Biol. 290 (1999) 615–625.
[15] M. Álvarez, T. Matomoros, L. Menéndez-Arias, Increased thermostability and fidelity of DNA synthesis of wild-type and mutant HIV-1 group O reverse transcriptases, J. Mol. Biol. 392 (2009) 872–884.
[16] G. Betancor, M.C. Puertas, M. Nevot, C. Garriga, M.A. Martínez, J. Martinez-Picado, L. Menéndez-Arias, Mechanisms involved in the selection of HIV-1 reverse transcriptase thumb subdomain polymorphisms associated with nucleoside analogue therapy failure, Antimicrob. Agents Chemother. 54 (2010) 4799–4811.
[17] G.L. Beilhartz, M. Wendeler, N. Baichoo, J. Rausch, S. Le Grice, M. Götte, HIV-1 reverse transcriptase can simultaneously engage its DNA/RNA substrate at both DNA polymerase and RNase H active sites: implications for RNase H inhibition, J. Mol. Biol. 388 (2009) 462–474.
[18] E. Nowak, W. Potrzebowski, P.V. Konarev, J.W. Rausch, M.K. Bona, D.I. Svergun, J.M. Bujnicki, S.F.J. Le Grice, M. Nowotny, Structural analysis of monomeric retroviral reverse transcriptase in complex with an RNA/DNA hybrid, Nucleic Acid Res. 41 (2013) 3874–3887.
[19] D. Lim, G.G. Gregorio, C. Bingman, E. Martinez-Hackert, W.A. Hendrickson, S.P. Goff, Crystal structure of the Moloney murine leukemia virus RNase H domain, J. Virol. 80 (2006) 8379–8389.
[20] D. Zhou, S. Chung, M. Miller, S.F.J. Le Grice, A. Wlodawer, Crystal structures of the reverse transcriptase-associated ribonuclease H domain of *Xenotropic murine* leukemia-virus related virus, J. Struct. Biol. 177 (2012) 638–645.
[21] A. Telesnitsky, S.P. Goff, RNase H domain mutations affect the interaction between Moloney murine leukemia virus reverse transcriptase and its primer–template, Proc. Natl. Acad. Sci. U.S.A. 329 (1993) 1276–1280.
[22] V. Barrioluengo, Y. Wang, S.F.J. Le Grice, L. Menéndez-Arias, Intrinsic DNA synthesis fidelity of xenotropic murine leukemia virus-related virus reverse transcriptase, FEBS J. 279 (2012) 1433–1444.
[23] E.R. Goedken, S. Marqusee, Metal binding and activation of the ribonuclease H domain from Moloney murine leukemia virus, Protein Eng. 12 (1999) 975–980.